









Nasopharyngeal metatranscriptome profiles of infants with bronchiolitis and risk of childhood asthma: a multicentre prospective study

Yoshihiko Raita ¹, Marcos Pérez-Losada^{2,3}, Robert J. Freishtat^{4,5,6}, Andrea Hahn ^{4,6,7}, Eduardo Castro-Nallar ⁸, Ignacio Ramos-Tapia⁸, Nathaniel Stearrett⁹, Yury A. Bochkov¹⁰, James E. Gern ^{10,11}, Jonathan M. Mansbach¹², Zhaozhong Zhu ¹, Carlos A. Camargo ¹ and Kohei Hasegawa¹

¹Dept of Emergency Medicine, Massachusetts General Hospital, Harvard Medical School, Boston, MA, USA. ²Dept of Biostatistics and Bioinformatics and Computational Biology Institute, The George Washington University, Washington, DC, USA. ³CIBIO-InBIO, Centro de Investigação em Biodiversidade e Recursos Genéticos, Universidade do Porto, Vairão, Portugal. ⁴Center for Genetic Medicine Research, Children's National Research Institute, Washington, DC, USA. ⁵Division of Emergency Medicine, Children's National Hospital, Washington, DC, USA. ⁶Dept of Pediatrics, The George Washington University School of Medicine and Health Sciences, Washington, DC, USA. ⁷Division of Infectious Diseases, Children's National Hospital, Washington, DC, USA. ⁸Centro de Bioinformática y Biología Integrativa, Universidad Andres Bello, Santiago, Chile. ⁹Computational Biology Institute, The George Washington University, Washington, DC, USA. ¹⁰Dept of Pediatrics, University of Wisconsin School of Medicine and Public Health, Madison, WI, USA. ¹¹Dept of Medicine, University of Wisconsin School of Medicine and Public Health, Madison, WI, USA. ¹²Dept of Pediatrics, Boston Children's Hospital, Harvard Medical School, Boston, MA, USA.

Corresponding author: Yoshihiko Raita (yraita1@alumni.jh.edu)



Shareable abstract (@ERSpublications)

This study suggests a complex interplay between respiratory virus, airway microbiome and host immune response in infants with severe bronchiolitis, and their integrated contributions to the subsequent development of childhood asthma <https://bit.ly/3xcM4ry>

Cite this article as: Raita Y, Pérez-Losada M, Freishtat RJ, *et al.* Nasopharyngeal metatranscriptome profiles of infants with bronchiolitis and risk of childhood asthma: a multicentre prospective study. *Eur Respir J* 2022; 60: 2102293 [DOI: 10.1183/13993003.02293-2021].

Abstract

Background Bronchiolitis is not only the leading cause of hospitalisation in US infants but also a major risk factor for asthma development. Growing evidence supports clinical heterogeneity within bronchiolitis. Our objectives were to identify metatranscriptome profiles of infant bronchiolitis, and to examine their relationship with the host transcriptome and subsequent asthma development.

Methods As part of a multicentre prospective cohort study of infants (age <1 year) hospitalised for bronchiolitis, we integrated virus and nasopharyngeal metatranscriptome (species-level taxonomy and function) data measured at hospitalisation. We applied network-based clustering approaches to identify metatranscriptome profiles. We then examined their association with the host transcriptome at hospitalisation and risk for developing asthma.

Results We identified five metatranscriptome profiles of bronchiolitis (n=244): profile A: virus^{RSV} microbiome^{commensals}, profile B: virus^{RSV/RV-A} microbiome^{H.influenzae}, profile C: virus^{RSV} microbiome^{S.pneumoniae}, profile D: virus^{RSV} microbiome^{M.nonliquefaciens}, and profile E: virus^{RSV/RV-C} microbiome^{M.catarrhalis}. Compared with profile A, profile B infants were characterised by a high proportion of eczema, *Haemophilus influenzae* abundance and enriched virulence related to antibiotic resistance. These profile B infants also had upregulated T-helper 17 and downregulated type I interferon pathways (false discovery rate (FDR) <0.005), and significantly higher risk for developing asthma (17.9% versus 38.9%; adjusted OR 2.81, 95% CI 1.11–7.26). Likewise, profile C infants were characterised by a high proportion of parental asthma, *Streptococcus pneumoniae* dominance, and enriched glycerolipid and glycerophospholipid metabolism of the microbiome. These profile C infants had an upregulated RAGE signalling pathway (FDR <0.005) and higher risk of asthma (17.9% versus 35.6%; adjusted OR 2.49, 95% CI 1.10–5.87).

Copyright ©The authors 2022.
For reproduction rights and permissions contact permissions@ersnet.org

This article has an editorial commentary:
<https://doi.org/10.1183/13993003.00378-2022>

Received: 20 Aug 2021
Accepted: 17 Nov 2021

Conclusions Metatranscriptome and clustering analysis identified biologically distinct metatranscriptome profiles that have differential risks of asthma.

Introduction

Bronchiolitis is the leading cause of hospitalisation in US infants, accounting for ~110 000 hospitalisations annually [1]. In addition to the substantial acute morbidity, ~30% of infants hospitalised for bronchiolitis (“severe bronchiolitis”) subsequently develop asthma [2]. However, the underlying mechanisms linking these two common conditions remain unclear. This major knowledge gap has hindered efforts to prevent asthma in this high-risk population.

Although bronchiolitis has traditionally been thought of as a single disease entity [3], growing evidence supports heterogeneity in the clinical manifestations [4] and pathobiology (*e.g.* as reflected by between-virus differences in the upper airway microbiome determined *via* 16S rRNA gene sequencing) [5–7]. Additionally, studies also suggest a complex interplay between viruses, microbiome and host response in the airway, and its interrelationship with respiratory health [2, 8–14]. Despite the clinical and research significance, no study has integrated virus and airway microbiome (both taxonomy and function) data to investigate the metatranscriptome profiles of bronchiolitis, their relationship with host response during the critical period of airway development (*i.e.* early infancy) and their contribution to incident asthma in later childhood.

To address this knowledge gap, we analysed data from a multicentre prospective cohort to 1) identify nasopharyngeal metatranscriptome profiles (or clusters) of bronchiolitis, and 2) investigate their association with the host airway response and subsequent development of asthma.

Methods

Study design, setting and participants

We analysed data from a multicentre prospective cohort study of infants hospitalised for bronchiolitis: the 35th Multicenter Airway Research Collaboration (MARC-35) study. Full details of the study design, setting, participants, data collection, testing and statistical analysis can be found in the supplementary material.

Briefly, at 17 sites across 14 US states (supplementary table S1), MARC-35 enrolled infants (age <1 year) who were hospitalised with an attending physician diagnosis of bronchiolitis during three bronchiolitis seasons in 2011–2014. The diagnosis of bronchiolitis was made according to the American Academy of Pediatrics bronchiolitis guidelines, defined as an acute respiratory illness with a combination of rhinitis, cough, tachypnoea, wheezing, crackles or chest retractions. We excluded infants with a pre-existing heart and lung disease, immunodeficiency, immunosuppression or gestational age <32 weeks, those with a previous bronchiolitis hospitalisation, or those who were transferred to a participating hospital >24 h after initial hospitalisation. All patients were treated at the discretion of the treating physicians. The Institutional Review Board at each participating hospital approved the study with written informed consent obtained from the parent or guardian.

Of 921 infants enrolled into the longitudinal cohort, the current analysis investigated 244 infants hospitalised for bronchiolitis who were randomly selected for nasopharyngeal metatranscriptome (microbiome) and transcriptome (host) testing (figure 1 and supplementary figure S1).

Data collection and measurement of virus, metatranscriptome and transcriptome

Clinical data (patient demographic characteristics, family, environmental and medical history, and details of the acute illness) were collected *via* structured interview and chart reviews using a standardised protocol. Additionally, nasopharyngeal airway specimens were collected within 24 h of hospitalisation using a standardised protocol [12]. Details of the data collection and measurement methods are described in the supplementary material. The nasopharyngeal specimens were tested for 1) respiratory viruses (*e.g.* respiratory syncytial virus (RSV) and rhinovirus (RV) species), 2) metatranscriptome (microbiome taxonomy at the species level and function) and 3) transcriptome (host function).

RNA sequencing for the nasopharyngeal dual transcriptome (metatranscriptome and transcriptome)

Full details of RNA extraction, RNA sequencing (RNAseq) and quality control are described in the supplementary material. Briefly, after total RNA extraction, DNase treatment and rRNA reduction, we performed RNAseq with an Illumina NovaSeq6000 using an S4 100PE Flowcell (Illumina, San Diego, CA, USA). All RNAseq samples had high sequence coverage (mean 8067019 paired-end reads per sample) after quality control. We filtered and trimmed raw reads for adapters and contaminants using the

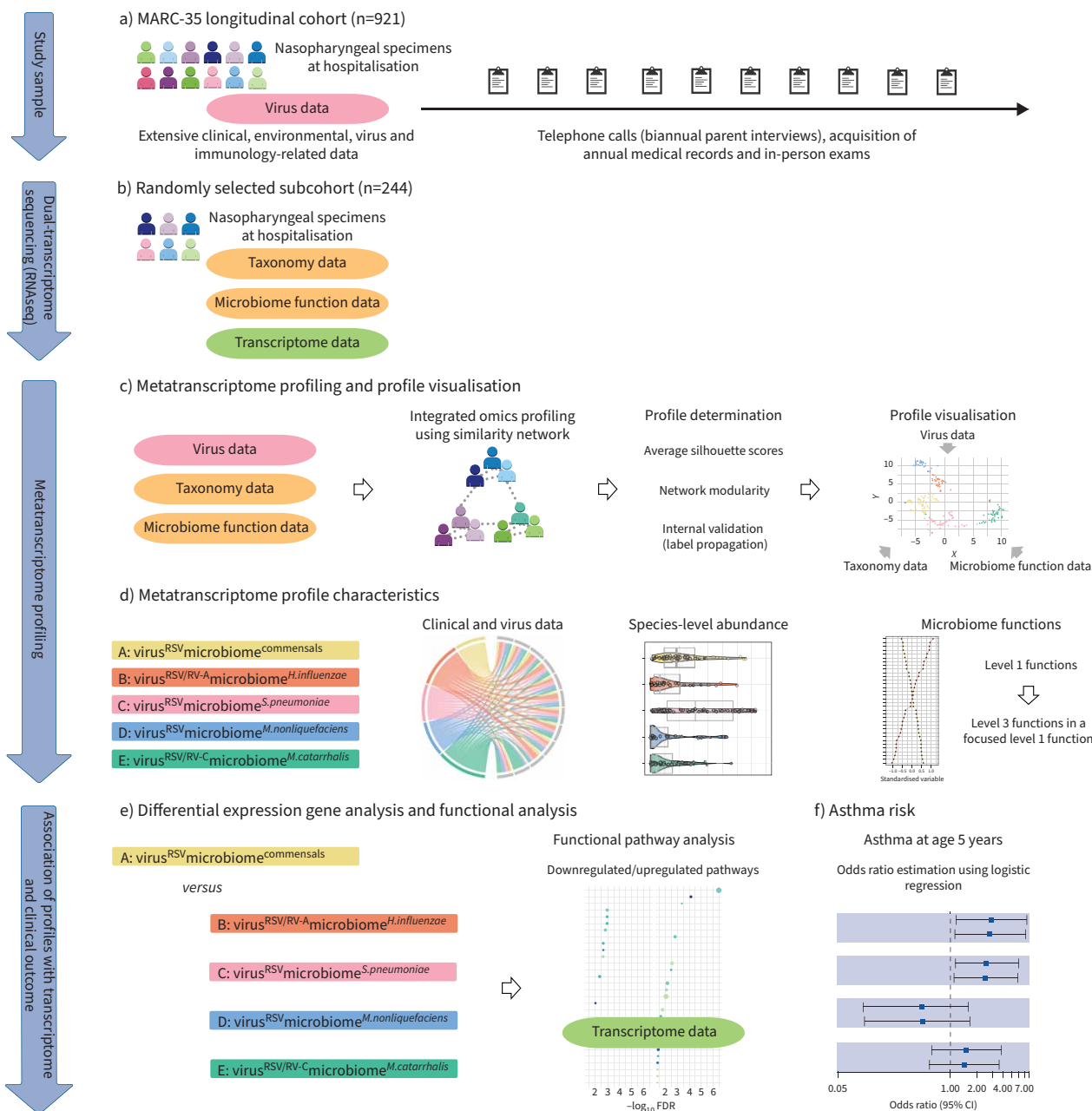


FIGURE 1 Analytic workflow of metatranscriptome profiling. **a)** A total of 921 infants (age <1 year) hospitalised with bronchiolitis comprised the 35th Multicenter Airway Research Collaboration (MARC-35) longitudinal cohort. At enrolment, the nasopharyngeal specimens were collected. These nasopharyngeal specimens were tested for respiratory viruses (e.g. respiratory syncytial virus (RSV) and rhinovirus (RV) species) and dual-transcriptome sequencing. These infants are followed with biannual parent interviews, acquisition of annual medical records and in-person exams. **b)** 244 randomly selected infants underwent dual-transcriptome sequencing (via RNA sequencing (RNAseq)) of nasopharyngeal specimens to characterise the microbiome taxonomy and function as well as the host transcriptome. **c)** After individually computing an affinity matrix for each of three datasets (i.e. virus, microbiome taxonomy and function data), we generated a fused affinity matrix by similarity network fusion. Then, we used the fused affinity matrix to identify metatranscriptome profiles by spectral clustering. To choose an optimal number of profiles, we used a combination of silhouette scores, network modularity, profile size, and clinical and biological plausibility. We visualised the five profiles by using the t-distributed stochastic neighbour embedding method. **d)** To visualise the between-metatranscriptome profile differences in the major clinical and virus variables, microbiome taxonomy, and functions, we used chord diagrams, pirate plots and ranked plots. **e)** To examine the relationship between the metatranscriptome profiles and host function (transcriptome data), we performed differential gene expression analyses and functional pathway analyses. As infants with profile A clinically resembled “classic” bronchiolitis and had the largest profile size, this group served as the reference group. **f)** To examine the relationship of the metatranscriptome profiles with the risk for developing asthma (binary outcome), we constructed unadjusted and adjusted logistic regression models. FDR: false discovery rate.

k-mers strategy in bbduck. We characterised the active (*via* RNA transcripts) bacterial component of the microbiome (species level) coupling PathoScope 2.0 with the expanded Human Oral Microbiome Database. To characterise microbiome function, we used SUPER-FOCUS and Diamond. To annotate proteins that implement a specific biological process or structural complex into subsystems, we used the SEED database. This database comprises three-level hierarchical microbiome functions: the level 1 subsystem with 35 functions, followed by the level 2 subsystem with 194 functions and the level 3 subsystem with 1290 functions. Lastly, we estimated host transcript abundances in Salmon using the human genome (hg38) and the mapping-based mode.

Functional and clinical outcomes

The outcomes of interest were 1) host function (the nasopharyngeal transcriptome) at index hospitalisation for bronchiolitis and 2) asthma development by age 5 years. The definition of asthma was based on a commonly used epidemiological definition of asthma: physician diagnosis of asthma by age 5 years plus either asthma medication use (*e.g.* albuterol inhaler, inhaled corticosteroids or montelukast) or asthma-related symptoms in the preceding year.

Statistical analysis

The objectives of the current study were 1) to identify biologically distinct metatranscriptome profiles among infants with bronchiolitis (description (clustering)), and 2) to relate them to the host transcriptome and risk of asthma development (association). The analytic workflow is summarised in figure 1. Full details of the statistical analysis can be found in the supplementary material.

Briefly, we first computed a distance matrix for each of the three datasets, *i.e.* virus (including the genomic load of RSV, RV-A and RV-C), microbiome taxonomy (species level) and microbiome function data: Euclidean distance for the virus data, Bray–Curtis distance for the taxonomy data and Pearson distance for the function data. Then, we computed an affinity matrix of each dataset separately and generated a fused affinity matrix by similarity network fusion using the SNFtool package. To identify mutually exclusive metatranscriptome profiles, we applied spectral clustering to the fused affinity matrix. To choose an optimal number of profiles, we used a combination of the silhouette scores (supplementary figure S2a), network modularity (supplementary figure S2b), profile size ($n=33\text{--}67$), and clinical and biological plausibility. The network modularity measures how well separated subnetworks are given a particular partitioning (*i.e.* profiles) of the network. To test the stability of profiles (*i.e.* internal validation), we computed the accuracy of profiles using semisupervised label propagation methods (supplementary figure S3). To complement these approaches, we also used *a priori* knowledge by confirming that the derived profiles were consistent with earlier studies [2].

After deriving the metatranscriptome profiles, we examined their relationships with both functional (host transcriptome) and clinical (asthma) outcomes. First, we conducted differential expression gene and functional pathway analyses by comparing the reference profile with each of the other profiles. To investigate whether genes for specific biological pathways were enriched among the large positive or negative fold changes, we conducted a functional class scoring analysis using the clusterProfiler package. Second, to determine the longitudinal association of the profiles with asthma at age 5 years (binary outcome), we constructed unadjusted and adjusted logistic regression models accounting for patient clustering within sites. In the sensitivity analysis, we examined the robustness of profile–outcome associations by repeating the analysis using a different number of profiles. We analysed the data using R version 3.6.1 (R Foundation for Statistical Computing, Vienna, Austria). All *p*-values were two-tailed, with $p<0.05$ considered statistically significant. We corrected for multiple testing using the Benjamini–Hochberg false discovery rate (FDR) method.

Results

Of the infants enrolled into this longitudinal cohort, the current study focused on 244 randomly selected infants with bronchiolitis who underwent testing for nasopharyngeal airway microbial metatranscriptome and host transcriptome (figure 1 and supplementary figure S1). The analytic cohort and non-analytic cohorts did not differ in patient characteristics ($p\geq 0.05$) (supplementary table S2), except for daycare use and solo-RSV infection. Among the analytic cohort, the median (interquartile range) age was 3 (2–6) months, 40.2% were female and 41.8% were non-Hispanic White. Overall, 91.0% were RSV infected, with solo-RSV infection in 65.2% and RSV/RV co-infection in 11.9% (table 1).

Integrated omics approach identified distinct metatranscriptome profiles

To derive biologically distinct metatranscriptome profiles of infant bronchiolitis, we applied integrative network and clustering approaches to the virus, microbiome taxonomy (species level) and microbiome

TABLE 1 Baseline characteristics and clinical course of infants with bronchiolitis, according to metatranscriptome profiles

	Overall	Profile A	Profile B	Profile C	Profile D	Profile E	p-value
Subjects	244 (100)	67 (27.5)	36 (14.8)	59 (24.2)	33 (13.5)	49 (20.1)	
Demographics							
Age (months)	3 (2–6)	3 (1–6)	4 (2–7)	3 (2–6)	4 (2–7)	3 (2–6)	0.36
Female	98 (40.2)	29 (43.3)	13 (36.1)	22 (37.3)	17 (51.5)	17 (34.7)	0.54
Race/ethnicity							0.33
Non-Hispanic White	102 (41.8)	29 (43.3)	14 (38.9)	21 (35.6)	16 (48.5)	22 (44.9)	
Non-Hispanic Black	57 (23.4)	12 (17.9)	6 (16.7)	21 (35.6)	8 (24.2)	10 (20.4)	
Hispanic	76 (31.1)	24 (35.8)	15 (41.7)	15 (25.4)	9 (27.3)	13 (26.5)	
Other or unknown	9 (3.7)	2 (3.0)	1 (2.8)	2 (3.4)	0 (0.0)	4 (8.2)	
Prematurity (32–36.9 weeks)	47 (19.3)	15 (22.4)	6 (16.7)	11 (18.6)	9 (27.3)	6 (12.2)	0.48
Birthweight (kg)	3.20 (2.89–3.57)	3.20 (2.90–3.52)	3.17 (2.70–3.42)	3.23 (2.86–3.69)	3.09 (2.79–3.43)	3.31 (3.00–3.64)	0.43
Caesarean delivery	84 (35.0)	19 (28.8)	15 (42.9)	22 (37.3)	11 (33.3)	17 (36.2)	0.69
Previous breathing problems (n)							0.92
0	204 (83.6)	55 (82.1)	31 (86.1)	50 (84.7)	27 (81.8)	41 (83.7)	
1	30 (12.3)	8 (11.9)	3 (8.3)	8 (13.6)	4 (12.1)	7 (14.3)	
2	10 (4.1)	4 (6.0)	2 (5.6)	1 (1.7)	2 (6.1)	1 (2.0)	
Previous ICU admission	4 (1.6)	3 (4.5)	0 (0.0)	0 (0.0)	1 (3.0)	0 (0.0)	0.19
History of eczema	31 (12.7)	3 (4.5)	8 (22.2)	10 (16.9)	2 (6.1)	8 (16.3)	0.03
Palivizumab use	8 (3.8)	1 (1.7)	2 (6.2)	3 (6.1)	0 (0.0)	2 (4.9)	0.48
Lifetime antibiotic use [#]	79 (32.4)	25 (37.3)	17 (47.2)	16 (27.1)	4 (12.1)	17 (34.7)	0.02
Ever attended daycare	71 (29.1)	15 (22.4)	11 (30.6)	16 (27.1)	13 (39.4)	16 (32.7)	0.46
Cigarette smoke exposure at home	34 (13.9)	9 (13.4)	4 (11.1)	11 (18.6)	6 (18.2)	4 (8.2)	0.52
Maternal smoking during pregnancy	34 (14.2)	9 (13.6)	7 (20.0)	7 (11.9)	3 (9.1)	8 (17.0)	0.69
Parental history of asthma	76 (31.1)	14 (20.9)	12 (33.3)	24 (40.7)	11 (33.3)	15 (30.6)	0.19
Parental history of eczema	46 (18.9)	9 (13.4)	12 (33.3)	12 (20.3)	8 (24.2)	5 (10.2)	0.06
Clinical presentation							
Weight (kg)	6.07 (4.60–7.99)	5.50 (4.36–7.10)	6.80 (5.16–8.12)	6.28 (4.52–7.53)	6.40 (4.75–8.20)	6.20 (4.80–8.45)	0.22
Respiratory rate (breaths·min ⁻¹)	48 (40–60)	48 (40–56)	48 (40–56)	48 (39–60)	52 (44–64)	50 (41–60)	0.45
Oxygen saturation							0.19
<90%	18 (7.6)	5 (7.9)	4 (11.8)	2 (3.4)	1 (3.1)	6 (12.2)	
90–93%	29 (12.2)	12 (19.0)	4 (11.8)	4 (6.8)	2 (6.2)	7 (14.3)	
≥94%	190 (80.2)	46 (73.0)	26 (76.5)	53 (89.8)	29 (90.6)	36 (73.5)	
Blood eosinophilia (≥4%)	21 (10.1)	4 (7.0)	4 (13.3)	5 (10.0)	2 (6.9)	6 (14.3)	0.73
IgE sensitisation	51 (20.9)	11 (16.4)	9 (25.0)	13 (22.0)	6 (18.2)	12 (24.5)	0.77
Clinical course							
Positive pressure ventilation use [¶]	18 (7.4)	6 (9.0)	3 (8.3)	5 (8.5)	3 (9.1)	1 (2.0)	0.55
Intensive treatment use [‡]	42 (17.2)	13 (19.4)	6 (16.7)	12 (20.3)	3 (9.1)	8 (16.3)	0.72
Length of stay (days)	2 (1–3)	2 (1–4)	2 (1–4)	2 (1–4)	2 (1–3)	2 (1–4)	0.89
Antibiotic use during hospitalisation	80 (32.8)	26 (38.8)	15 (41.7)	19 (32.2)	8 (24.2)	12 (24.5)	0.29
Corticosteroid use during hospitalisation	29 (11.9)	8 (11.9)	7 (19.4)	10 (16.9)	1 (3.0)	3 (6.1)	0.11
Respiratory virus							
RSV infection	222 (91.0)	61 (91.0)	31 (86.1)	59 (100.0)	33 (100.0)	38 (77.6)	<0.001
RSV-A [§]	153 (62.7)	46 (68.7)	22 (61.1)	41 (69.5)	15 (45.5)	29 (59.2)	0.15
RSV-B [§]	71 (29.1)	16 (23.9)	9 (25.0)	19 (32.2)	18 (54.5)	9 (18.4)	0.01
Solo-RSV infection	159 (65.2)	42 (62.7)	21 (58.3)	48 (81.4)	24 (72.7)	24 (49.0)	0.007
RV infection							
RV-A	26 (10.7)	8 (11.9)	7 (19.4)	5 (8.5)	2 (6.1)	4 (8.2)	0.41
RV-B	4 (1.6)	1 (1.5)	1 (2.8)	0 (0.0)	1 (3.0)	1 (2.0)	0.67
RV-C	21 (8.6)	2 (3.0)	0 (0.0)	1 (1.7)	2 (6.1)	16 (32.7)	<0.001
Solo-RV infection	13 (5.3)	4 (6.0)	1 (2.8)	0 (0.0)	0 (0.0)	8 (16.3)	0.002
RSV/RV co-infection	29 (11.9)	5 (7.5)	3 (8.3)	6 (10.2)	5 (15.2)	10 (20.4)	0.25
Other co-infection pathogens with RSV [†]	34 (13.9)	14 (20.9)	7 (19.4)	5 (8.5)	4 (12.1)	4 (8.2)	0.17
Chronic outcome							
Asthma at age 5 years	62 (25.4)	12 (17.9)	14 (38.9)	21 (35.6)	3 (9.1)	12 (24.5)	0.009

Data are presented as n (%) or median (interquartile range), unless otherwise stated; percentages may not total 100% due to rounding and missing data. ICU: intensive care unit; RSV: respiratory syncytial virus; RV: rhinovirus. [#]: any systemic antibiotic use from birth up to the index hospitalisation for bronchiolitis; [¶]: infants with bronchiolitis who underwent continuous positive airway ventilation and/or mechanical ventilation; [‡]: infants with bronchiolitis who were admitted to the ICU and/or who underwent positive pressure ventilation; [§]: two infants had co-infection of RSV-A and RSV-B; [†]: infants with co-infection of RSV and non-RV pathogens, including adenovirus (n=7), bocavirus (n=8), endemic coronavirus (n=15), enterovirus (n=1), influenza virus (n=1), human metapneumovirus (n=4), *Mycoplasma pneumoniae* (n=1) and parainfluenza virus (n=3) (since six infants had co-infection with three or more infecting agents, the total number is not equal to 34).

function data (figure 1). Both the average silhouette scores and network modularity found that a five-class model was the optimal fit (supplementary figure S2), with the five profiles called A, B, C, D and E. The semisupervised label propagation methods also indicated that the stability was also highest with the five-class model (supplementary figure S3).

The five distinct metatranscriptome profiles (figure 2a and supplementary figure S4) were chiefly characterised by the identified virus(es) and the major bacteria species of the nasopharyngeal airway microbiome: profile A: virus^{RSV} microbiome^{commensals} (27.5%); profile B: virus^{RSV/RV-A} microbiome^{H.influenzae} (14.8%); profile C: virus^{RSV} microbiome^{S.pneumoniae} (24.2%); profile D: virus^{RSV} microbiome^{M.nonliquefaciens} (13.5%); and profile E: virus^{RSV/RV-C} microbiome^{M.catarrhalis} (20.1%) (table 1, and figures 2b and 3).

Descriptively, infants with profile A were characterised by a young age, a low proportion of parental asthma and eczema and personal history of eczema, and a high proportion of RSV infection (figures 2 and supplementary figures S5–S7). In many respects they resembled “classic” bronchiolitis. These infants also had a higher abundance of commensals (e.g. *Corynebacterium* and *Cutibacterium*; both FDR <0.001) (figure 3 and supplementary figure S7). Infants with profile B were characterised by a high proportion of lifetime antibiotics use, history of eczema, parental eczema, IgE sensitisation and co-infection with RV-A, and a higher abundance of *Haemophilus influenzae* (FDR <0.001 when compared with those with profile A). Infants with profile C were characterised by a high proportion of parental asthma and solo-RSV infection as well as a higher abundance of *Streptococcus pneumoniae* (FDR <0.001). Infants with profile D were characterised by a low proportion of hypoxaemia, a high proportion of RSV infection and a higher abundance of *Moraxella nonliquefaciens* (FDR <0.001). Infants with profile E were characterised by a high proportion of RV-C co-infection and a higher abundance of *Moraxella catarrhalis* (FDR <0.001). These virus and microbiome variables that characterised the profiles had high-ranked normalised mutual information scores, indicating large contributions to the similarity network (supplementary figure S8).

Metatranscriptome profiles had distinct microbiome function pathways

These metatranscriptome profiles of infant bronchiolitis also had distinct microbiome functions. For example, compared with infants with profile A (virus^{RSV} microbiome^{commensals}) who clinically resembled “classic” bronchiolitis and were the largest group, those with profile B (virus^{RSV/RV-A} microbiome^{H.influenzae}) had enriched virulence and iron acquisition and metabolism (FDR <0.05) (figure 4). More specifically, profile B infants had an upregulated virulence function related to antibiotic resistance (e.g. multidrug resistance efflux pumps) (FDR <0.05) (supplementary figure S9a) and iron metabolism function related to haemin transport (FDR <0.05) (supplementary figure S9b). Profile C (virus^{RSV} microbiome^{S.pneumoniae}) infants had enriched fatty acid, lipid and isoprenoid metabolism (FDR <0.05) (figure 4), e.g. upregulated glycerolipid and glycerophospholipid metabolism (FDR <0.05) (supplementary figure S10). In contrast, profile D (virus^{RSV} microbiome^{M.nonliquefaciens}) infants had downregulated glycerolipid and glycerophospholipid function in fatty acid, lipid and isoprenoid metabolism (FDR <0.05) (figure 4 and supplementary figure S11). Lastly, profile E (virus^{RSV/RV-C} microbiome^{M.catarrhalis}) infants had upregulated stress response metabolism (FDR <0.05) (figure 4), e.g. cold shock CspA protein family (FDR <0.05) (supplementary figure S12).

Metatranscriptome profiles had distinct host transcriptome characteristics during infancy and differential risk for developing asthma

To better understand the relationship between the metatranscriptome profiles and the host response (represented by the transcriptome) during infancy, we conducted differential expression gene and functional pathway analyses. Compared with profile A, profile B had 63 differentially enriched pathways (FDR <0.05) (supplementary figure S13), e.g. upregulated T-helper 17 (Th17) and downregulated type I interferon (IFN) pathways. Similarly, profile C had 45 differentially enriched pathways (FDR <0.05), e.g. an upregulated RAGE (receptor for advanced glycation end-products) signalling pathway (supplementary figure S14). For profiles A versus D and A versus E comparisons, the detailed differences are summarised in supplementary figures S15 and S16.

The metatranscriptome profiles also had differential risks for developing asthma by age 5 years (figure 5). For example, compared with profile A infants, profile B infants had a significantly higher risk of asthma (17.9% versus 38.9%; adjusted OR 2.81, 95% CI 1.11–7.26; p=0.030). Likewise, profile C infants also had a significantly higher risk of asthma (35.6%; adjusted OR 2.49, 95% CI 1.10–5.87; p=0.031), while profile D infants had a non-significantly lower risk of asthma (9.1%; adjusted OR 0.47, 95% CI 0.10–1.65; p=0.28). In the stratification by development of recurrent wheeze by age 3 years, the results were similar (supplementary figure S17).

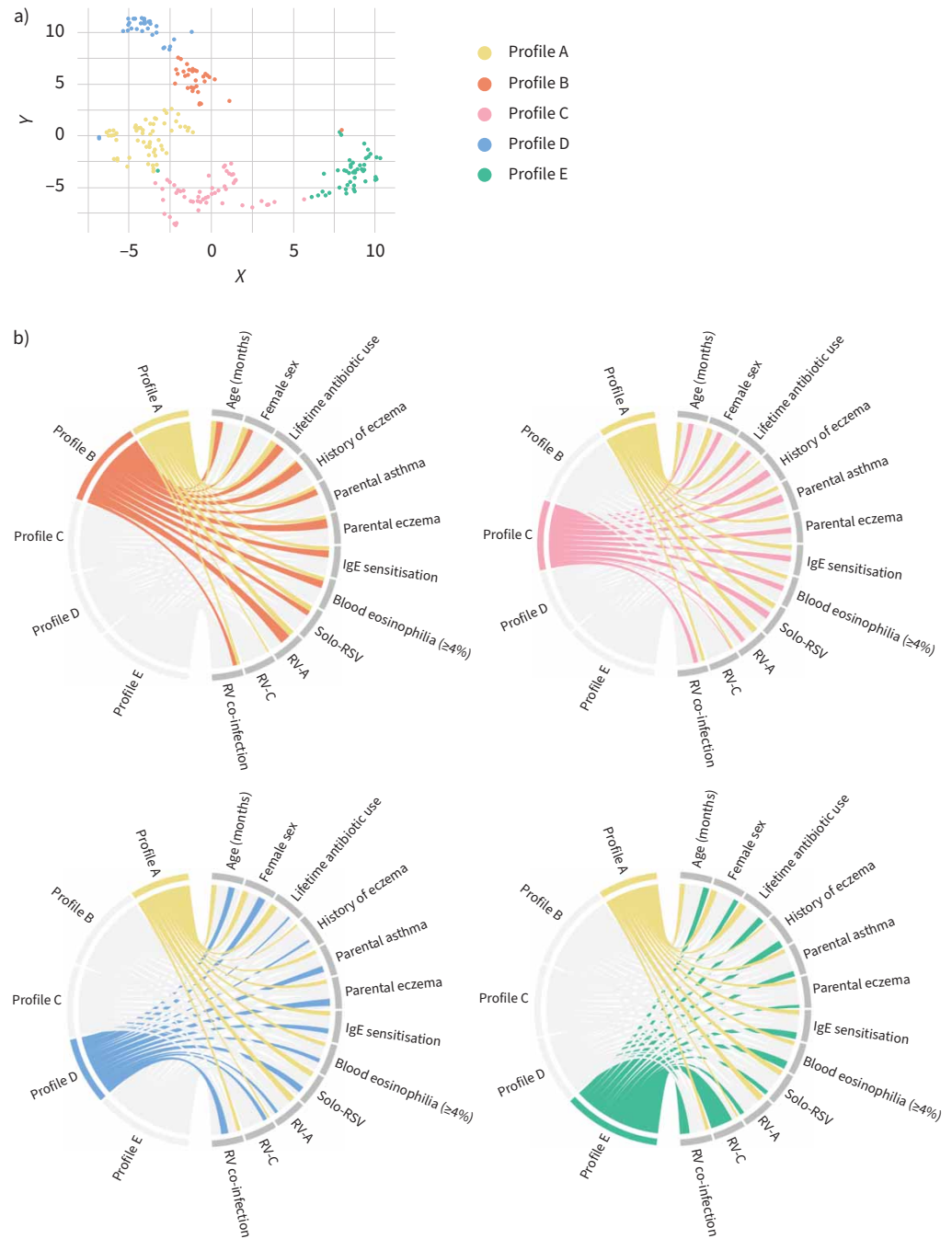


FIGURE 2 Metatranscriptome profiles among infants with bronchiolitis, and their relationship with major clinical and virus variables. **a)** t-distributed stochastic neighbour embedding (t-sne) of nasopharyngeal metatranscriptome profiles. To visualise the metatranscriptome profiles, the t-sne method was applied to the five eigenvectors in the spectral clustering. Each dot represents the metatranscriptome of a single infant in a low-dimensional space. The infants cluster together according to their metatranscriptome profiles. **b)** Major clinical and virus characteristics according to metatranscriptome profiles. The ribbons connect from the individual metatranscriptome profiles to the major clinical and virus characteristics. The width of the ribbon represents the proportion of infants within the profile who have the corresponding clinical or virus characteristic, which was scaled to a total of 100%. For example, the profile B infants (orange) had a high proportion of lifetime antibiotics use, history of eczema, parental eczema, IgE sensitisation, blood eosinophilia and co-infection with rhinovirus (RV)-A. Profile C (pink) infants had a high proportion of parental asthma and solo-respiratory syncytial virus (RSV) infection.

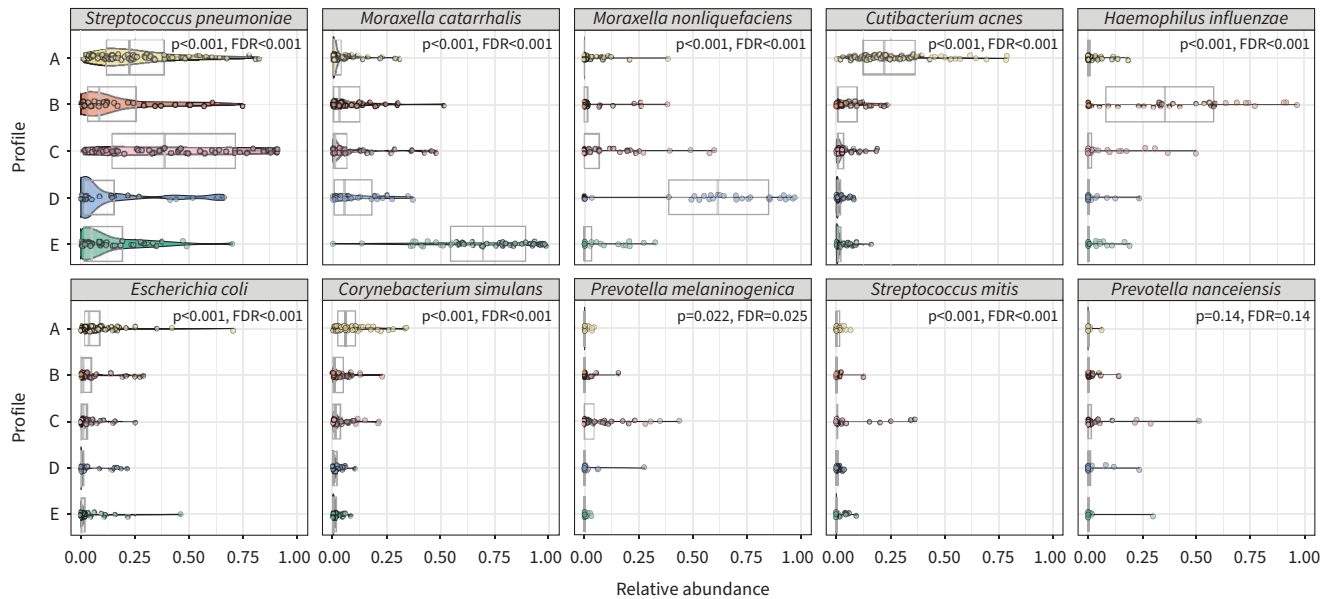


FIGURE 3 Between-profile differences in relative abundance of the 10 most abundant nasopharyngeal microbial species among infants with bronchiolitis. The pirate plots (a combination of box plots and violin plots) show the distribution of the 10 most abundant species in the nasopharyngeal microbiome, according to the five metatranscriptome profiles. The box plots show median and interquartile range. In the overlying violin plots, the width represents the probability that infants in a profile take on a specific relative abundance. The between-profile differences in the relative abundance were tested by the Kruskal–Wallis test. FDR: false discovery rate.

Sensitivity analysis

To address the robustness of these findings, we examined different numbers of profiles. The alluvial plot (supplementary figure S18) demonstrates the consistency of the original profiles (profiles A–E) across the different numbers chosen (four and six profiles). For example, with the use of four-class models (that had the second-highest accuracy in label propagation methods), the first and fourth profiles had >90% concordance with the original profiles A and E (supplementary table S3). In contrast, the second profile had a mixture of the original profiles B and C. Similar to the primary analysis, these four profiles were also characterised by virus and microbiome taxonomy (e.g. *S. pneumoniae* and *M. catarrhalis*) (supplementary table S3 and supplementary figure S19). Lastly, compared with profile 1 (which is concordant with profile A), profile 2 (concordant with profiles B and C) infants with distinct microbiome functions (e.g. enriched by virulence, iron acquisition and metabolism, and fatty acid, lipid and isoprenoid metabolism; supplementary figure S20) had upregulated Th17 (FDR=0.002) and RAGE signalling (FDR=0.001) pathways. These infants also had a significantly higher risk for developing asthma (18.8% versus 34.6%; adjusted OR 2.25, 95% CI 1.05–5.00; $p=0.041$) (supplementary figure S21).

Discussion

By integrating virus and nasopharyngeal metatranscriptome (both microbiome taxonomy and function) data from a multicentre prospective cohort study of 244 infants with severe bronchiolitis, we identified five biologically distinct metatranscriptome profiles. In particular, infants with profile B (virus^{RSV/RV-A} microbiome^{*H. influenzae*}) not only had distinct microbiome function (e.g. upregulated virulence function) but also were associated with a unique host response in the nasopharyngeal airway (e.g. upregulated Th17 pathways) at the time of bronchiolitis. Additionally, infants with profile C (virus^{RSV} microbiome^{*S. pneumoniae*}) also had a distinctive microbiome function (e.g. enriched lipid metabolism) and host response (e.g. upregulated RAGE signalling pathway). Furthermore, these two metatranscriptome profiles had a significantly higher risk for developing childhood asthma. To the best of our knowledge, this is the first study that has identified metatranscriptome profiles in bronchiolitis and demonstrated their relationship with the host airway response and subsequent development of asthma.

Recent research has suggested the relationship between virus, airway microbiome, host response and respiratory disease. For example, studies have reported the association between respiratory viruses and a unique upper airway microbiome (measured either *via* 16S rRNA gene sequencing or quantitative PCR) in infants with bronchiolitis [5, 6, 15] and school-age children [16]. In these studies, RV-A infection was

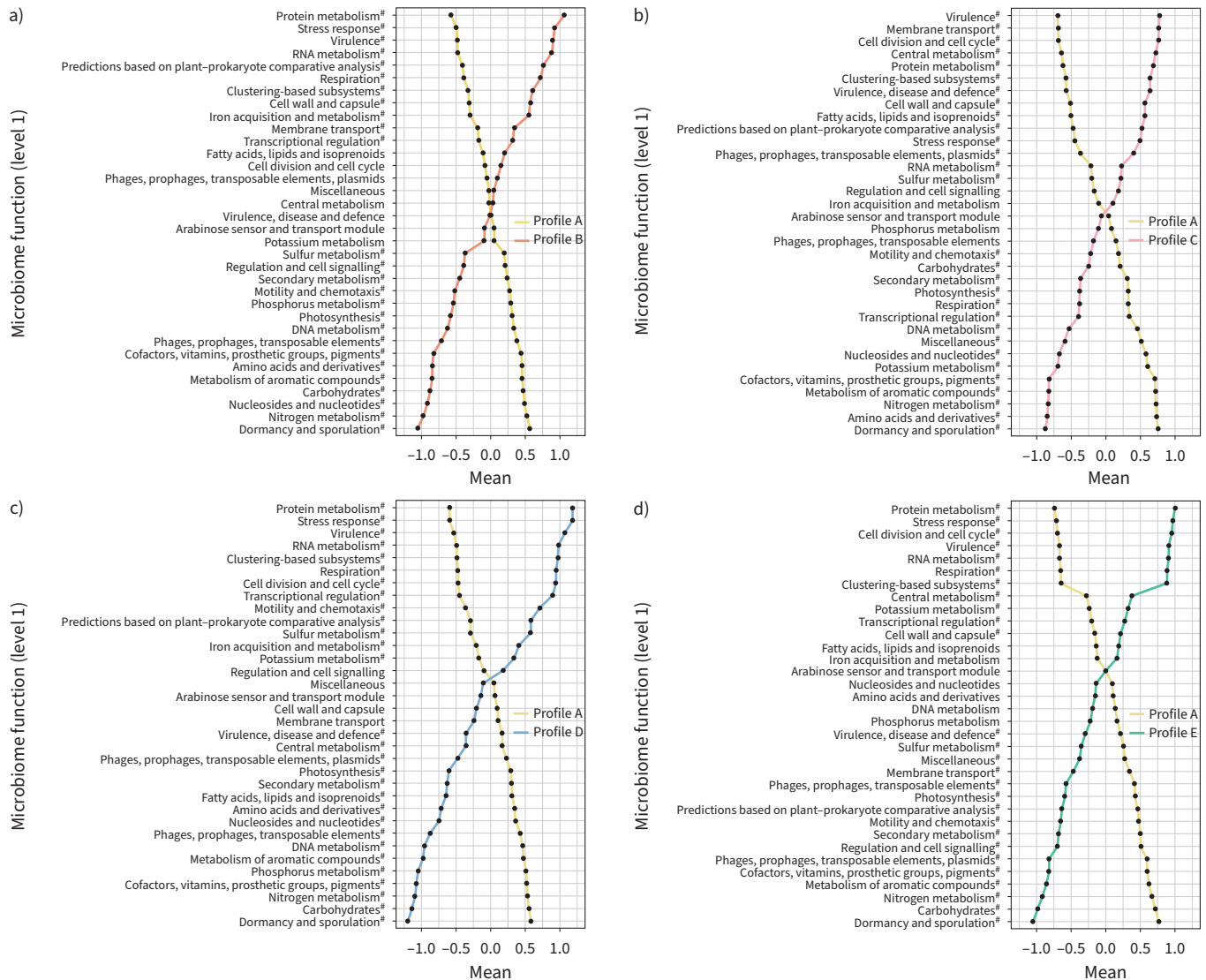


FIGURE 4 Between-profile differences in nasopharyngeal microbiome function among infants with bronchiolitis. In all comparisons (metatranscriptome profile A versus a) profile B, a) profile C, c) profile D and d) profile E), the mean values of microbiome function variables (35 level 1 functions) in the corresponding profiles are plotted. The microbiome function variables are standardised by using auto-scaling after variance stabilising transformation. The differences in more detailed microbiome functions (level 3 functions) of specific level 1 functions are presented in supplementary figures S9–S12. #: false discovery rate <0.05.

associated with a *Haemophilus*-dominant profile and RV-C with a *Moraxella*-dominant profile, which is consistent with our metatranscriptomics findings. Recent studies have also shown the potential role of *Haemophilus* and *Streptococcus* genera in the upper airway, both among infants with or without bronchiolitis, in the host immune response [17, 18] and the development of wheeze illness and asthma [18–20]. Furthermore, research has suggested that the interaction of microbiome–host functions, via downstream metabolic regulation, contributes to the pathobiology of bronchiolitis and asthma [21]. Indeed, studies of the upper airway metabolome among infants with bronchiolitis have reported the associations of altered lipid metabolism with disease severity [12] and asthma risk [21]. The current study corroborates these earlier reports, and extends them not only by identifying metatranscriptome profiles through the integrated omics approach but also by demonstrating their relationship with the unique host immune response and asthma development.

There are several potential mechanisms linking the metatranscriptome profiles to the host airway response and subsequent asthma risk. First, we observed the relationship of profile B (virus^{RSV/RV-A} microbiome^{H.influenzae}), characterised by a high likelihood of previous antibiotics exposure, atopy/allergic

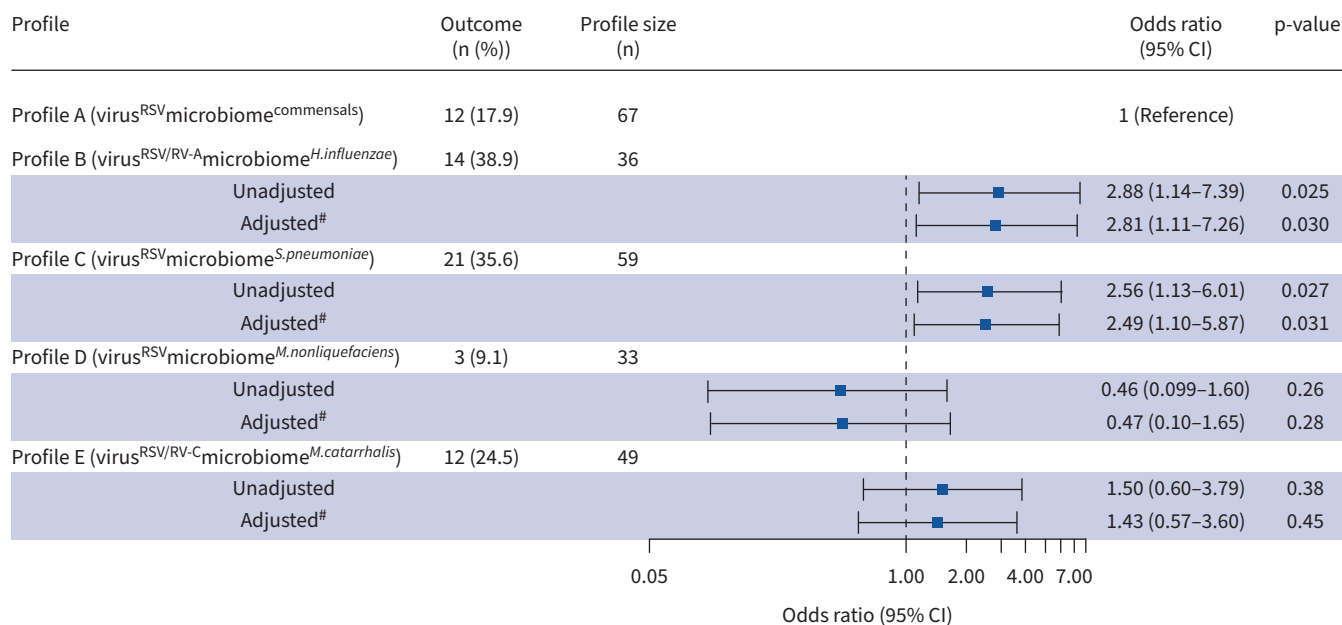


FIGURE 5 Association between nasopharyngeal metatranscriptome profiles of infant bronchiolitis and risk for developing asthma. Asthma (binary outcome) was defined as physician diagnosis of asthma at age 5 years plus either asthma medication use (e.g. albuterol inhaler, inhaled corticosteroids or montelukast) or asthma-related symptoms in the preceding year. To examine the association between bronchiolitis profiles (profile A as the reference) and the risk of developing childhood asthma, unadjusted and adjusted logistic regression models were fit. #: multivariable random effects logistic model adjusted for age, sex and clustering within hospitals. RSV: respiratory syncytial virus; RV: rhinovirus.

sensitisation, *H. influenzae* abundance, and enriched virulence related with antibiotic resistance and iron metabolism function, with upregulated Th17 and downregulated type I IFN pathways. Consistently, studies have reported that antibiotic exposures during early infancy lead to *Haemophilus*-dominant maturation of the nasal microbiome during the first 2 years of life [22]. Likewise, RV-A infection is also associated with a high abundance of *Haemophilus* in young children [7, 16]. Additionally, *H. influenzae* requires haemin transport function and X factor for its aerobic growth [23]. Furthermore, animal models have reported that *H. influenzae* induces early interleukin-17 responses from lung macrophages and neutrophils, followed by later responses from Th17 cells in lungs and mediastinal lymph nodes, leading to neutrophil influx into the airways [24]. Studies have also shown roles of the Th17 pathway in neutrophilic inflammation, steroid insensitivity and airway remodelling in both allergic and non-allergic asthma [25, 26]. In addition to the upregulated Th17 pathway, profile B also had downregulated type I IFN pathways. Recent research has reported immature type I IFN response to RV-A infection [27]. Reduced antiviral response (e.g. IFNs) to RV infection impairs phagocytosis of *H. influenzae* among patients with chronic lung disease [28]. Studies have also demonstrated that the type I IFN response to RV infection is impaired among infants with allergic sensitisation [29], and that the use of anti-IgE monoclonal antibody improves the IFN- α response and reduces asthma exacerbation risks [30]. These prior data are in line with our findings in profile B.

Second, the mechanisms linking profile C (virus^{RSV}microbiome^{S.pneumoniae}), characterised by a high likelihood of solo-RSV infection, *S. pneumoniae* dominance, and enriched glycerolipid and glycerophospholipid metabolism, to the unique host response (e.g. RAGE signalling) and asthma risk warrants further clarification. Research has shown that RSV infection increases the virulence of *S. pneumoniae* [31]. *S. pneumoniae* produces phosphatidic acid, a precursor to all membrane glycerophospholipids [32]. Studies have also suggested the pro-inflammatory role of glycerophospholipid (e.g. activation of natural killer T-cells) in the pathobiology of asthma [33, 34]. Additionally, *S. pneumoniae* is associated with upregulated RAGE expression in the lung [35]. A Mendelian randomisation study has also demonstrated the causal role of RAGE in asthma pathobiology [36]. Furthermore, compared with RAGE knockout mice, wild-type mice develop more pronounced airway inflammation and mucus metaplasia when intranasally administered recombinant type 2 cytokines [37]. While it is intriguing to observe the abundance of *S. pneumoniae* and its potential pathobiological effect in the post-pneumococcal conjugate vaccine (PCV) era, research has shown that the introduction of PCV-13 has led to changes in pneumococcal serotypes, genotypes and antimicrobial resistance [38].

In contrast, we observed that profile D (virus^{RSV}microbiome^{*M.nonliquefaciens*}) was characterised by downregulated glycerolipid and glycerophospholipid function, and had the lowest risk for developing asthma. Studies have reported that *M. nonliquefaciens* is less pathogenic [39] and associated with a lower risk of incident asthma [40]. Besides, the low bronchiolitis severity (suggested by the low proportion of hypoxaemia) in profile D may have also contributed to the decreased asthma risk. Lastly, profile E (virus^{RSV/RV-C}microbiome^{*M.catarrhalis*}) had upregulated CspA family proteins, which induce *uspAI* gene expression and prolong survival of *M. catarrhalis* [41]. *M. catarrhalis*'s lipopolysaccharides activate both MyD88-dependent and TRIF-dependent signalling pathways [42]. These pathways activate pro-inflammatory downstream signalling factors (e.g. NF-κB, mitogen-activated protein kinases and IFN regulatory factors) that play roles in asthma [43]. Notwithstanding the complexity of these mechanisms, the observed interrelations between the metatranscriptome profiles, host immune response and asthma development are important findings. Our data should not only advance research that will disentangle the complex web but they also inform the development of microbiome (or endotype)-specific strategies for the primary prevention of asthma.

Our study has several potential limitations. First, bronchiolitis involves inflammation of the lower airways in addition to the upper airways. While the present study is based on nasopharyngeal samples, studies have shown that upper airway sampling provides a reliable representation of the lung microbiome [43] and transcriptome [44]. Furthermore, the use of upper airway specimens is preferable because lower airway sampling (e.g. bronchoscopy) would be quite invasive in young infants. Second, the nasopharyngeal samples were obtained at a single time-point. While longitudinal molecular data are also informative, the study objective was to identify metatranscriptome profiles of bronchiolitis. However, even with single-time-point data, we successfully identified biologically distinct profiles that are longitudinally associated with asthma risk. Third, it is possible that asthma diagnosis was misclassified and that some children will go on to develop asthma at a later age. To address these points, the study sample is currently being followed up to age 9 years. Fourth, the present study did not have healthy "controls". However, our study objective was not to evaluate metatranscriptome profiles related to bronchiolitis development (i.e. bronchiolitis yes versus no) but to examine the relationship between the metatranscriptome profile of infants with bronchiolitis and their asthma risk. Fifth, while this hypothesis-generating study derives novel and well-calibrated hypotheses that facilitate future experiments, our findings warrant further validation. Lastly, the study sample consisted of racially/ethnically and geographically diverse infants hospitalised for bronchiolitis. Our findings may not be generalisable to infants with mild-to-moderate bronchiolitis or a sample with different respiratory virus proportions. Regardless, our data remain relevant for the ~110 000 infants hospitalised yearly in the USA [1], a vulnerable population with substantial morbidity burden.

Conclusions

In summary, by applying an integrated omics approach to data from a multicentre prospective cohort of 244 infants with severe bronchiolitis, we identified five biologically distinct and clinically meaningful metatranscriptome profiles. These profiles were associated not only with distinct host airway responses during bronchiolitis but also with differential risks for developing asthma. Our data suggest a complex interplay between respiratory virus, airway microbiome and host immune response, and their integrated contributions to the subsequent development of asthma. For clinicians, our findings may provide an evidence base for the early identification of high-risk children during an important period of airway development, i.e. early infancy. For researchers, our data should facilitate further investigations into the development of microbiome profile (or endotype)-specific strategies for asthma prevention.

Acknowledgements: We thank the MARC-35 study hospitals and research personnel for their ongoing dedication to bronchiolitis and asthma research (supplementary table S1), and Ashley F. Sullivan and Janice A. Espinola (Massachusetts General Hospital, Boston, MA, USA) for their many contributions to the MARC-35 study. We also thank Alkis Togias (National Institutes of Health, Bethesda, MD, USA) for helpful comments about the study results.

Conflict of interest: Y. Raita has nothing to disclose. M. Pérez-Losada has nothing to disclose. R.J. Freishtat has nothing to disclose. A. Hahn has nothing to disclose. E. Castro-Nallar has nothing to disclose. I. Ramos-Tapia has nothing to disclose. N.I. Stearrett has nothing to disclose. Y.A. Bochkov has patents on production methods of rhinoviruses. J.E. Gern is a paid consultant to AstraZeneca and Meissa Vaccines Inc., has stock options in Meissa Vaccines Inc., and has patents on production methods of rhinoviruses. J.M. Mansbach has nothing to disclose. Z. Zhu has nothing to disclose. C.A. Camargo has nothing to disclose. K. Hasegawa has nothing to disclose.

Support statement: This study was supported by grants from the National Institutes of Health (NIH): U01 AI-087881, R01 AI-114552, R01 AI-108588, R01 AI-134940 and UG3/UH3 OD-023253. M. Pérez-Losada was partially

supported by the Margaret Q. Landenberger Research Foundation, the NIH National Center for Advancing Translational Sciences (UL1 TR-001876) and the Fundação para a Ciência e a Tecnologia (T495756868-00032862). The content of this manuscript is solely the responsibility of the authors and does not necessarily represent the official views of the NIH. The funding organisations were not involved in the collection, management or analysis of the data; preparation or approval of the manuscript; or decision to submit the manuscript for publication. Funding information for this article has been deposited with the Crossref Funder Registry.

References

- 1 Fujiogi M, Goto T, Yasunaga H, *et al.* Trends in bronchiolitis hospitalizations in the United States: 2000–2016. *Pediatrics* 2019; 144: e20192614.
- 2 Hasegawa K, Dumas O, Hartert TV, *et al.* Advancing our understanding of infant bronchiolitis through phenotyping and endotyping: clinical and molecular approaches. *Expert Rev Respir Med* 2016; 10: 891–899.
- 3 Ralston SL, Lieberthal AS, Meissner HC, *et al.* Clinical practice guideline: the diagnosis, management, and prevention of bronchiolitis. *Pediatrics* 2014; 134: e1474–e1502.
- 4 Dumas O, Hasegawa K, Mansbach JM, *et al.* Severe bronchiolitis profiles and risk of recurrent wheeze by age 3 years. *J Allergy Clin Immunol.* 2019; 143: 1371–1379.
- 5 Rosas-Salazar C, Shilts MH, Tovchigrechko A, *et al.* Differences in the nasopharyngeal microbiome during acute respiratory tract infection with human rhinovirus and respiratory syncytial virus in infancy. *J Infect Dis* 2016; 214: 1924–1928.
- 6 Mansbach JM, Hasegawa K, Henke DM, *et al.* Respiratory syncytial virus and rhinovirus severe bronchiolitis are associated with distinct nasopharyngeal microbiota. *J Allergy Clin Immunol* 2016; 137: 1909–1913.
- 7 Toivonen L, Camargo CA, Gern JE, *et al.* Association between rhinovirus species and nasopharyngeal microbiota in infants with severe bronchiolitis. *J Allergy Clin Immunol* 2019; 143: 1925–1928.
- 8 Rosas-Salazar C, Shilts MH, Tovchigrechko A, *et al.* Nasopharyngeal *Lactobacillus* is associated with a reduced risk of childhood wheezing illnesses following acute respiratory syncytial virus infection in infancy. *J Allergy Clin Immunol* 2018; 142: 1447–1456.
- 9 Turi KN, Shankar J, Anderson LJ, *et al.* Infant viral respiratory infection nasal immune-response patterns and their association with subsequent childhood recurrent wheeze. *Am J Respir Crit Care Med* 2018; 198: 1064–1073.
- 10 Raita Y, Camargo CA, Bochkov YA, *et al.* Integrated-omics endotyping of infants with rhinovirus bronchiolitis and risk of childhood asthma. *J Allergy Clin Immunol* 2021; 147: 2108–2117.
- 11 Hasegawa K, Mansbach JM, Ajami NJ, *et al.* The relationship between nasopharyngeal CCL5 and microbiota on disease severity among infants with bronchiolitis. *Allergy* 2017; 72: 1796–1800.
- 12 Stewart CJ, Mansbach JM, Wong MC, *et al.* Associations of nasopharyngeal metabolome and microbiome with severity among infants with bronchiolitis. A multiomic analysis. *Am J Respir Crit Care Med* 2017; 196: 882–891.
- 13 Fujiogi M, Camargo CA, Raita Y, *et al.* Association of rhinovirus species with nasopharyngeal metabolome in bronchiolitis infants: a multicenter study. *Allergy* 2020; 75: 2379–2383.
- 14 Tang HHF, Lang A, Teo SM, *et al.* Developmental patterns in the nasopharyngeal microbiome during infancy are associated with asthma risk. *J Allergy Clin Immunol* 2021; 147: 1683–1691.
- 15 Stewart CJ, Mansbach JM, Piedra PA, *et al.* Association of respiratory viruses with serum metabolome in infants with severe bronchiolitis. *Pediatr Allergy Immunol* 2019; 30: 848–851.
- 16 Bashir H, Grindle K, Vrtis R, *et al.* Association of rhinovirus species with common cold and asthma symptoms and bacterial pathogens. *J Allergy Clin Immunol* 2018; 141: 822–824.
- 17 Følsgaard NV, Schjørring S, Chawes BL, *et al.* Pathogenic bacteria colonizing the airways in asymptomatic neonates stimulates topical inflammatory mediator release. *Am J Respir Crit Care Med* 2013; 187: 589–595.
- 18 Larsen JM, Brix S, Thysen AH, *et al.* Children with asthma by school age display aberrant immune responses to pathogenic airway bacteria as infants. *J Allergy Clin Immunol* 2014; 133: 1008–1013.
- 19 Mansbach JM, Luna PN, Shaw CA, *et al.* Increased *Moraxella* and *Streptococcus* species abundance after severe bronchiolitis is associated with recurrent wheezing. *J Allergy Clin Immunol* 2020; 145: 518–527.
- 20 Bisgaard H, Hermansen MN, Buchvald F, *et al.* Childhood asthma after bacterial colonization of the airway in neonates. *N Engl J Med* 2007; 357: 1487–1495.
- 21 Fujiogi M, Camargo CA, Raita Y, *et al.* Integrated associations of nasopharyngeal and serum metabolome with bronchiolitis severity and asthma: a multicenter prospective cohort study. *Pediatr Allergy Immunol* 2021; 32: 905–916.
- 22 Raita Y, Toivonen L, Schuez-Havupalo L, *et al.* Maturation of nasal microbiota and antibiotic exposures during early childhood: a population-based cohort study. *Clin Microbiol Infect* 2021; 27: 283.e1–283.e7.
- 23 Whitby PW, Seale TW, VanWagoner TM, *et al.* The iron/heme regulated genes of *Haemophilus influenzae*: comparative transcriptional profiling as a tool to define the species core modulon. *BMC Genomics* 2009; 10: 6.
- 24 Essilfie A-T, Simpson JL, Horvat JC, *et al.* *Haemophilus influenzae* infection drives IL-17-mediated neutrophilic allergic airways disease. *PLoS Pathog* 2011; 7: e1002244.

- 25 Chesné J, Braza F, Mahay G, *et al.* IL-17 in severe asthma. Where do we stand? *Am J Respir Crit Care Med* 2014; 190: 1094–1101.
- 26 Ricciardolo FLM, Sorbello V, Folino A, *et al.* Identification of IL-17F/frequent exacerbator endotype in asthma. *J Allergy Clin Immunol* 2017; 140: 395–406.
- 27 Wark PAB, Grissell T, Davies B, *et al.* Diversity in the bronchial epithelial cell response to infection with different rhinovirus strains. *Respirology* 2009; 14: 180–186.
- 28 Finney LJ, Belchamber KBR, Fenwick PS, *et al.* Human rhinovirus impairs the innate immune response to bacteria in alveolar macrophages in chronic obstructive pulmonary disease. *Am J Respir Crit Care Med* 2019; 199: 1496–1507.
- 29 Durrani SR, Montville DJ, Pratt AS, *et al.* Innate immune responses to rhinovirus are reduced by the high-affinity IgE receptor in allergic asthmatic children. *J Allergy Clin Immunol* 2012; 130: 489–495.
- 30 Teach SJ, Gill MA, Togias A, *et al.* Preseasonal treatment with either omalizumab or an inhaled corticosteroid boost to prevent fall asthma exacerbations. *J Allergy Clin Immunol* 2015; 136: 1476–1485.
- 31 Smith CM, Sandrini S, Datta S, *et al.* Respiratory syncytial virus increases the virulence of *Streptococcus pneumoniae* by binding to penicillin binding protein 1a. A new paradigm in respiratory infection. *Am J Respir Crit Care Med* 2014; 190: 196–207.
- 32 Gullett JM, Cuypers MG, Frank MW, *et al.* A fatty acid-binding protein of *Streptococcus pneumoniae* facilitates the acquisition of host polyunsaturated fatty acids. *J Biol Chem* 2019; 294: 16416–16428.
- 33 Fazlollahi M, Lee TD, Andrade J, *et al.* The nasal microbiome in asthma. *J Allergy Clin Immunol* 2018; 142: 834–843.
- 34 Kinjo Y, Wu D, Kim G, *et al.* Recognition of bacterial glycosphingolipids by natural killer T cells. *Nature* 2005; 434: 520–525.
- 35 van Zoelen MAD, Schouten M, de Vos AF, *et al.* The receptor for advanced glycation end products impairs host defense in pneumococcal pneumonia. *J Immunol* 2009; 182: 4349–4356.
- 36 Raita Y, Zhu Z, Freishtat RJ, *et al.* Soluble receptor for advanced glycation end products (sRAGE) and asthma: Mendelian randomisation study. *Pediatr Allergy Immunol* 2021; 32: 1100–1103.
- 37 Perkins TN, Oczypok EA, Dutz RE, *et al.* The receptor for advanced glycation end products is a critical mediator of type 2 cytokine signaling in the lungs. *J Allergy Clin Immunol* 2019; 144: 796–808.
- 38 Lo SW, Gladstone RA, van Tonder AJ, *et al.* Pneumococcal lineages associated with serotype replacement and antibiotic resistance in childhood invasive pneumococcal disease in the post-PCV13 era: an international whole-genome sequencing study. *Lancet Infect Dis* 2019; 19: 759–769.
- 39 LaCroce SJ, Wilson MN, Romanowski JE, *et al.* *Moraxella nonliquefaciens* and *M. osloensis* are important *Moraxella* species that cause ocular infections. *Microorganisms* 2019; 7: 163.
- 40 Raita Y, Pérez-Losada M, Freishtat RJ, *et al.* Integrated omics endotyping of infants with respiratory syncytial virus bronchiolitis and risk of childhood asthma. *Nat Commun* 2021; 12: 3601.
- 41 Heiniger N, Spaniol V, Troller R, *et al.* A reservoir of *Moraxella catarrhalis* in human pharyngeal lymphoid tissue. *J Infect Dis* 2007; 196: 1080–1087.
- 42 Hassan F. Molecular mechanisms of *Moraxella catarrhalis*-induced otitis media. *Curr Allergy Asthma Rep* 2013; 13: 512–517.
- 43 Marsh RL, Kaestli M, Chang AB, *et al.* The microbiota in bronchoalveolar lavage from young children with chronic lung disease includes taxa present in both the oropharynx and nasopharynx. *Microbiome* 2016; 4: 37.
- 44 Poole A, Urbanek C, Eng C, *et al.* Dissecting childhood asthma with nasal transcriptomics distinguishes subphenotypes of disease. *J Allergy Clin Immunol* 2014; 133: 670–678.